Available online at www.sciencedirect.com
SCIENCE DIRECT®
Diamond & Related Materials 15 (2006) 870 – 874
DIAMOND AND RELATED MATERIALS
www.elsevier.com/locate/diamond

The effect of Schottky barrier lowering and nonplanar emitter geometry on the performance of a thermionic energy converter

J.R. Smith [a,*], R.J. Nemanich [a], G.L. Bilbro [b]

[a] Department of Physics, North Carolina State University, Raleigh, NC 27695-8202, USA
[b] Department of Electrical and Computer Engineering, North Carolina State University, Raleigh, NC 27695, USA

Available online 24 February 2006

Abstract

An extension of the classical model of thermionic emission was developed to include the effects of nonplanar emitter surfaces and Schottky barrier lowering (SBL) on the output of a thermionic energy converter (TEC). Nonplanar emitter geometries along with Schottky barrier lowering may be useful in increasing both the maximum output power and output current of a thermionic energy converter. The finite element method was used to calculate the enhanced normal electric field at the surface of an emitter coated with an ultra-nanocrystalline diamond (UNCD) film and patterned with field enhancing tips. The result was used to determine the local enhanced output current and power. For the geometries considered the increased surface area of the emitter plays a significant role in increasing the output power and output current. Moreover, a calculation of the single electron time of flight shows that electrons traveling through a field enhanced region of the interelectrode space might spend half as long in transit, thus helping to mitigate the negative space charge effect that degrades the performance of vacuum TECs.

Keywords: Diamond properties and applications; Thermionic energy conversion; Schottky barrier lowering; Field enhancement

1. Introduction

Thermionic electron emission is the process of electron emission from a material being held at a finite temperature. This phenomenon may be employed in a device known as a thermionic energy converter (TEC) which is a type of heat engine which converts heat directly into electrical work. Planar vacuum thermionic energy converters have been studied for some time as a means of converting heat directly into electrical energy. These devices have the advantage over mechanical generators of containing no moving parts. Detailed theories of planar vacuum TECs have been described by Hatsopoulos and Gyftopoulos [1,2] and Dugan [3] in order to provide a way to analyze their typical performance. Despite the maturity of the theory, conventional vacuum TECs were unable to generate appreciable power below an operating temperature of about 1200 K and as a result have been relegated to specialized applications.

There are two main phenomena that affect the performance of a vacuum thermionic energy converter: electron emission from the electrodes, and electron transport in the interelectrode space, also known as the negative space charge phenomenon. Structures on the surface of the emitter will locally increase the electric field, which will in turn locally decrease the work function of the emitter by Schottky barrier lowering (SBL). The lower work function will result in a higher emission current. The purpose of this study is to investigate the effect that SBL has on the output current and the performance of a vacuum TEC.

The operation of a planar TEC is described by a motive diagram shown in Fig. 1A. In the standard operating mode, electrons with thermal energy greater than the vacuum level of the emitter escape the emitter material and travel across the interelectrode space where they are collected by the collector. This net electron current can be used to do work in an external load. At the tip of a field enhancing structure on the emitter surface, the motive drops rapidly with distance, thereby reducing the emission barrier for electrons via SBL. Fig. 1B shows the motive diagram in this case.

This study is motivated by the recent experimental measurements of thermionic emission from nitrogen doped

* Corresponding author. NC State University Department of Physics, Campus Box 8202, Raleigh, NC 27695-8202, USA. Tel.: +1 919 515 2474; fax: +1 919 513 0670.
E-mail address: jrsmith3@ncsu.edu (J.R. Smith).

0925-9635/$ - see front matter © 2006 Elsevier B.V. All rights reserved.
doi:10.1016/j.diamond.2005.12.057

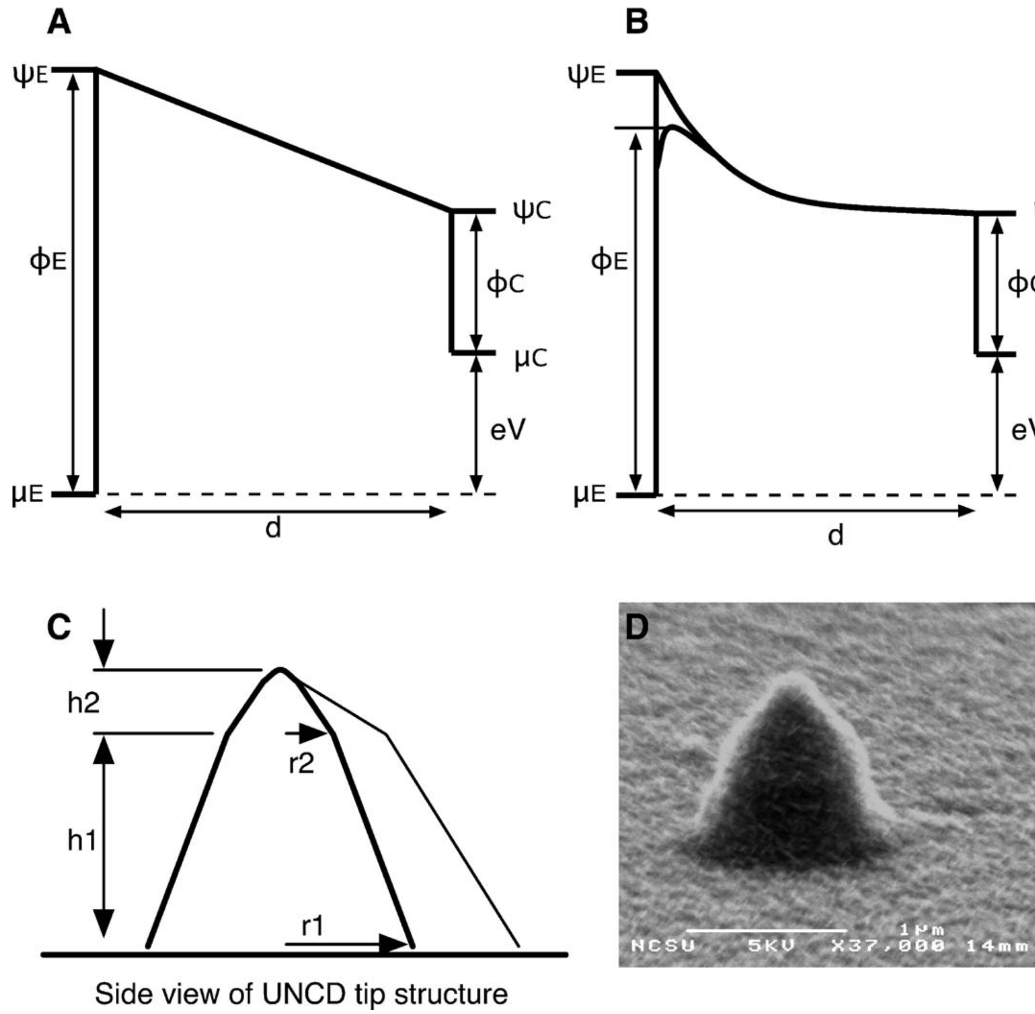

Fig. 1. A. Motive diagram of TEC in normal operating conditions where ψ is the vacuum level, ϕ is the work function, μ is the Fermi level, and V is the output voltage. The subscripts 'E' and 'C' denote emitter and collector, respectively. B. Motive diagram of TEC showing the effect of SBL on emission barrier. C. Schematic of tip structures including dimension lines with geometric parameter labels. The sharp tip is shown to scale in bold, the blunt tip is shown in the thin line. D. SEM of the UNCD coated Si tip [5].

diamond films [4] and from surfaces with an array of tips coated with N-doped, ultrananocrystalline (UNCD) diamond film [5]. Other studies have been completed to study the field emission of diamond at elevated temperatures [6] and the field emission of diamond nanostructures [7] in order to understand possible energy conversion applications of these materials. The donor level of single substitutional nitrogen in diamond is typically found at 1.7 eV below the conduction band minimum. Thus, at elevated temperatures, a barrier to emission of less than 1.7 eV could be expected. As a result, N-doped diamond could be an ideal, low work function material for use in a TEC. The reported thermionic emission from N-doped diamond films suggest that a work function of less than 2.0 eV may be obtained. Moreover, the emission from the UNCD coated tips was more intense at the tip apex indicating enhanced emission intensity [5].

In order to achieve appreciable power output from a TEC operating at lower temperatures, the emitter and collector surfaces must have low work functions. As noted above, recent studies have employed nitrogen doped diamond as a low work function material, [4] as well as employing field enhancing nanostructures on the emitter surface in order to further reduce the work function via SBL [5]. The model that was developed was based on the model of a vacuum TEC described in [1] which has planar electrodes, ignores space charge and collector back emission, and regards electron current to be positive. For the collector temperatures considered in this study (300 K), back emission is negligible and therefore is ignored in the model to avoid unnecessary complication. Typically, for low emission current densities and closely spaced electrodes, the negative space charge effect is not appreciable. Studies have been completed to calculate the negative space charge effect for more complex boundary conditions [8], but to avoid unnecessary complications the model presented here neglects this effect.

When an accelerating field is present outside an electrode, the barrier for electron emission is lowered by an amount $\Delta\psi$ [9]. The Richardson–Dushman equation ($J_{\mathrm{RD}}=AT^2$ exp

$(-\phi/kT)$) is modified to account for this barrier lowering as given in Eq. (1).

$$J = AT^2 \exp\left(-\frac{\varphi - \Delta\psi}{kT}\right) \quad (1)$$

where

$$\Delta\psi = e^2\left(\frac{eE}{16\pi\varepsilon_0}\right)^{1/2}$$

and A is Richardson's constant (120 A/cm^2 K^2), T is the electrode temperature (K), ϕ is the work function of the electrode (eV), k is Boltzmann's constant (8.62×10^{-5} eV/K), e is the fundamental charge, E is the local electric field strength (V/cm) at the surface of the emitter, and ε_0 is the permittivity of free space (8.85×10^{-14} F/cm).

In this study, a model to determine the benefit of SBL on the output current density of a vacuum TEC is developed along the lines described above. Specifically, the model is implemented to calculate the emission current from UNCD coated Si tip structures as described in [5] and shown in Fig. 1D.

2. Model description

In this section, we present a general description of the model used to describe the effect that nonplanar emitter geometries and SBL have on the output current density of a thermionic energy converter. For this model, the following additional assumptions beyond of the planar model are imposed. First, the emission current density from the emitter is directed normal to the surface, and is given by the Richardson–Dushman equation with the SBL modification as in Eq. (1); second, all current that is emitted from the emitter travels across the interelectrode space and is collected at the collector.

As with the planar models, only those electrons with energy sufficient to overcome the maximum potential barrier contribute to the output current. As the load increases, the voltage of the collector increases with respect to the emitter and as a result the barrier over which electrons must pass to escape the emitter material increases. At some voltage, the barrier height of the emitter is at the same level as the barrier of the collector. This point is referred to as the contact voltage and is given by $V=(\phi_E-\phi_C)/e$. For voltages greater than the contact voltage, field enhancement effects at the emitter are no longer significant because emitted electrons would have to climb a potential hill to the collector. Furthermore, the output current density drops off rapidly with voltages greater than the contact voltage. Therefore, the model does not consider voltages greater than the contact voltage.

To calculate the effect that SBL has on the output current density, the electric field at the surface of the emitter must be calculated by solving Laplace's equation with the correct boundary conditions. Since a specific emitter geometry is employed, the solution was approximated using the finite element method with the help of the software package FEMLAB. In order to simplify the problem, the geometry of the TEC was sectioned into the smallest symmetric pieces, referred to as cells. The boundary conditions for the emitter and collector are determined by ϕ_E, ϕ_C, and the electrode output voltage, V. Smaller values of V mean a greater potential difference in the interelectrode space and as a result, a greater electric field at the emitter surface. For a particular set of ϕ_E, ϕ_C, and V, the potential at the emitter was set to a value of ϕ_E/e, and the potential at the collector to a value of $\phi_C/e+V$. Since the walls of the cell are planes of symmetry, the boundary conditions were set such that the normal displacement field was zero across the boundary.

FEMLAB can calculate the surface charge density, σ, on an external boundary. The electrostatic boundary condition $\sigma=n_2(D_1-D_2)$ with the assumption that $D=0$ inside the emitter, and the constitutive relation $D=\varepsilon_0 E$ yields an expression for E normal to and at the surface of the emitter: $E=\sigma/\varepsilon_0$. In this way, the value of the normal electric field was approximated at points on the surface of the emitter. Once the normal electric field strength has been determined at the surface of the emitter, the local enhanced emission current density can be determined at all points on the emitter surface using Eq. (1).

Once the SBL enhanced current has been determined at all points on the emitter surface, the result is integrated over the floor of the cell, then divided by the area of the footprint of the cell (A_{fp}) as in Eq. (2). This result is an effective output current density (J_{eff}) that can be compared to the output current density of the planar case.

$$J_{eff} = \frac{1}{A_{fp}}\int J_{floor} d^2\Omega \quad (2)$$

There are two reasons why the emission current density in the nonplanar emitter case is higher than the emission current density in the planar emitter case. First, the overall surface area of the emitter is greater in the nonplanar case than the planar case. Second, SBL locally enhances the emission current at the tip structures. If one ignores the effect SBL has on the emission current, substituting the Richardson–Dushman equation (J_{RD}) into Eq. (2) yields the effective emission current density due to the increased emitter surface area, given by Eq. (3).

$$J_{eff} = \frac{A_{np}}{A_{fp}} J_{RD} \quad (3)$$

To calculate the enhanced effective emission current including SBL, the procedure described above must be followed to calculate the SBL enhanced current on the emitter surface, then the emission current is integrated as in Eq. (2).

3. Implementation

To calculate the output current density as a function of voltage, the following procedure was applied. First, the geometry in question was generated, the boundary conditions were set as described above, and the electrostatic potential was approximated via the finite element method. The normal electric field was calculated according to the derivation above, and the effective output current was calculated according to Eq. (2). Different values of the output voltage, V, were used to determine the output current characteristics.

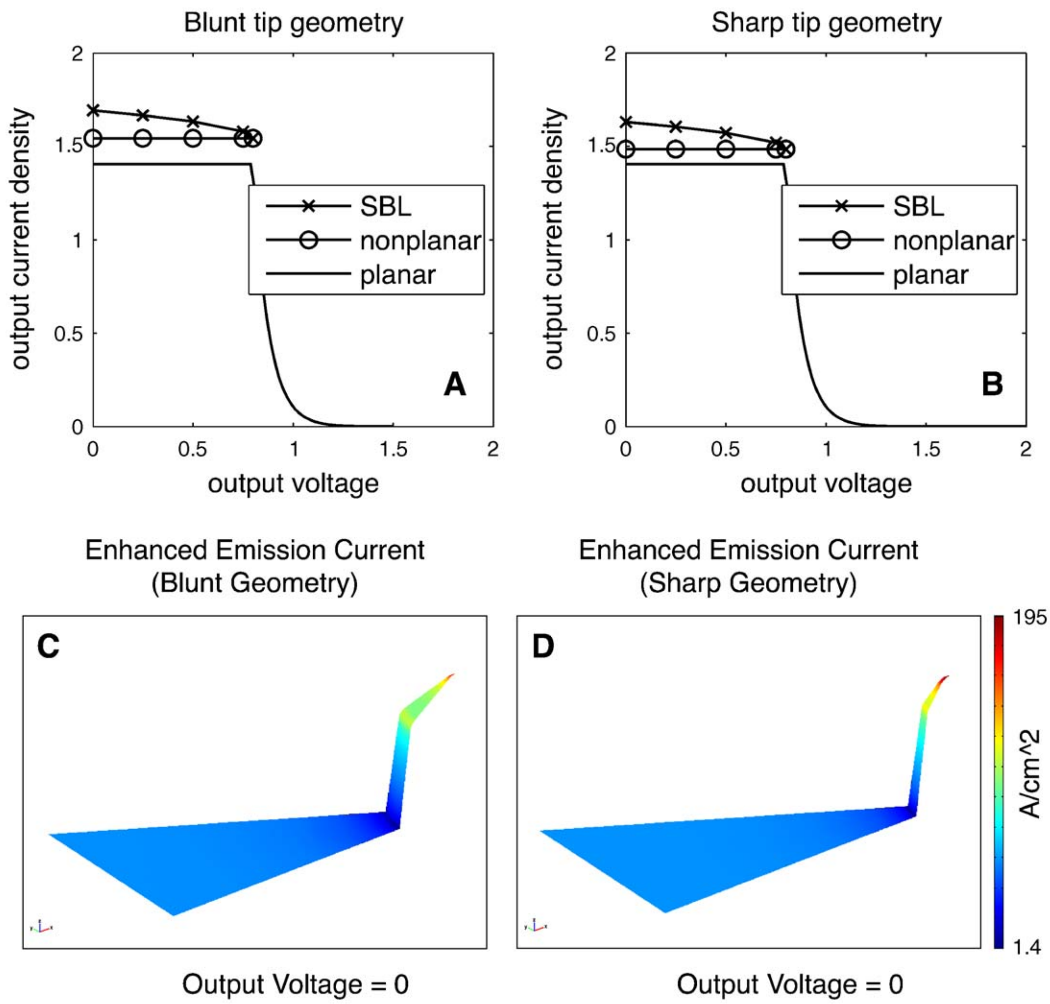

Fig. 2. Results of output current characteristics calculations and finite element calculations. A and B show the output current characteristics of both the SBL output current density and the planar output current density for the blunt and sharp tip geometries, respectively. C and D show the results of the finite element calculations of local output current on the tip structures for blunt and sharp tip geometries, respectively.

Two different geometry configurations were considered: tips that were more blunt, and tips that were more sharp. Fig. 1C shows a diagram of the geometric parameter labels of the tip structures. The sharp structures had geometric parameters r1 = 0.3 μm, r2 = 0.2 μm. The blunt structures had r1 = 0.5 μm, and r2 = 0.4 μm. For both blunt and sharp tips, h1 = 0.8 μm and h2 = 0.3 μm, respectively. The structures were arranged in a regular hexagonal pattern on the surface of the emitter such that the tips were 5 μm apart from their nearest neighbor, measured from the tip apex. The emitter temperature was taken to be 950 K, the emitter work function was taken to be 1.4 eV, and the collector work function was taken as 0.6 eV. The emitter and collector were spaced 5 μm apart from emitter base to collector surface. The apex of both tip geometries was rounded and had a radius of curvature of 100 nm.

4. Results and discussion

Output current characteristics measured in A/cm^2 for the blunt and sharp tip cases are given in Fig. 2A and B. In each graph, the output current characteristic is given for the planar case, the nonplanar case which ignores SBL, and the nonplanar case including SBL. The SBL enhanced current is greatest at zero voltage. In the case of the blunt tips, the overall enhanced current density is increased over the planar current density by a factor of up to 1.21, and increased by a factor of 1.10 by the increased emitter surface area alone. In the sharp case, the overall output current density is increased by a factor of up to 1.16, and increased by a factor of 1.06 by the increased emitter surface area alone. The output current density for the blunt geometry is slightly higher than the output current density of the sharp geometry because the overall surface area of the blunt tipped emitter is higher than that of the sharp tipped emitter.

For both geometries, the enhanced output current at points on the emitter surface of the cell is shown in Fig. 2C and D. At zero voltage the maximum enhanced output current density is located at the apex of the tip. In the case of the sharp geometry, the enhanced current density has a value of 1.937 A/cm^2, whereas the blunt geometry the value is 1.877 A/cm^2. In the planar case, the corresponding unenhanced emission current density is 1.405 A/cm^2. Thus, the maximum enhanced emission current from the sharp tip is 38% higher than the planar case and the blunt tip is 34% higher than the planar case.

From the previous results, it is evident that there are competing effects contributing to the increase in output current from nanostructured emitter surfaces. The blunter tips result in more overall surface area and thus more overall emission current, but less locally enhanced emission current. The converse is true about sharper tips. It is possible to increase the density of tips on the surface in order to retain tip sharpness and increase surface area, but at some point occlusion of emitted electrons by nearby structures will occur which will decrease the overall output current density. Furthermore, dense structures will screen one another from high electric fields thereby decreasing the emission enhanced by SBL. The problem of finding the optimum structure geometry and density to maximize output current from increased surface area and enhanced emission from SBL will be necessary to fully understand the benefit of these effects on the performance of vacuum TECs. Similar experimental [10] and theoretical [11] studies have been completed to determine the field screening effect that carbon nanotubes have on one another in carbon nanotube field emission arrays.

Electrons emitted in a region of higher electric field will experience a more rapid increase of kinetic energy than those electrons in a region of lower electric field. Single electron kinematics calculations indicate that electrons in a low electric field will spend up to twice as long in the interelectrode space compared to the electrons in a higher field. Thus, in the regions of high electric field near the tips of the structures, electrons will move much more quickly across the interelectrode space, reducing the number of electrons in the space and therefore reducing the negative space charge effect.

Any reduction of the negative space charge effect has two implications. First, the TEC will perform more closely to the idealized case described in this study. Second, space charge reduction relaxes the constraints on interelectrode distance: larger, more easily manufactured interelectrode distances become feasible as a result of space charge mitigation. The full benefits of the effect of field enhancing structures on space charge mitigation will become clear only when a fully three-dimensional model of electron transport in the interelectrode space is developed.

5. Summary and conclusions

A model to calculate the effect of field enhancing structures and Schottky barrier lowering on the output current of a vacuum thermionic energy conversion device was developed. This model ignored the effects of collector back emission and the negative space charge effect since both effects were negligible in the specific case studied. Nitrogen doped diamond has a low emission barrier height and is thus an attractive choice for an emitter material. According to the model, the output current density of a TEC with a nonplanar emitter is increased over that of the planar emitter due to two effects: the increased emitter surface area, and SBL. The problem of optimizing feature sharpness and density to determine and optimal geometric configuration to maximize output current remains to be solved, but is now available through this model. Structures on the emitter surface clearly have an effect on the negative space charge phenomenon, but the quantitative analysis requires a fully three-dimensional electron transport model.

Acknowledgments

This research was supported by the Office of Naval Research through the MURI on Thermionic Energy Conversion.

References

[1] G. Hatsopoulous, E. Gyftopoulous, Thermionic Energy Conversion, vol. 1, MIT Press, Cambridge, 1973.
[2] G. Hatsopoulous, E. Gyftopoulous, Thermionic Energy Conversion, vol. 2, MIT Press, Cambridge, 1979, p. 350.
[3] A. Dugan, J. Appl. Phys. 31 (8) (1960) 1397.
[4] F.A.M. Koeck, J.M. Garguilo, R.J. Nemanich, Diamond Relat. Mater. 13 (2004) 2052.
[5] J.M. Garguilo, F.A.M. Koeck, R.J. Nemanich, X.C. Xiao, J.A. Carlisle, O. Auciello, Phys. Rev., B 72 (1) (2005) 165404.
[6] S.H. Shin, T.S. Fisher, D.G. Walker, A.M. Strauss, W.P. Kang, J.L. Davidson, J. Vac. Sci. Technol., B 21 (1) (2003) 587.
[7] T.S. Fisher, D.G. Walker, J. Heat Transfer 124 (2002) 954.
[8] A.R. Knox, A. Asenov, A.C. Lowe, Solid-State Electron. 45 (2001) 841.
[9] W. Schottky, Phys. Z. 15 (1914) 872.
[10] J.S. Suh, K.S. Jeong, J.S. Lee, I. Han, App. Phys. Lett. 80 (2002) 239.
[11] X.Q. Wang, M. Wang, Z.H. Li, Y.B. Xu, P.M. He, Ultramicroscopy 102 (2005) 181.